AIAA JOURNAL
Vol. 34, No. 6, June 1996

Improved Theory for Contact Indentation of Sandwich Panels

Robin Olsson* and Hugh L. McManus†
Massachusetts Institute of Technology, Cambridge, Massachusetts 02139-4307

Core crushing and large face-sheet deflections are incorporated in a theory for contact indentation of sandwich panels. The model is based on the assumption of axisymmetric indentation of an infinite elastic face sheet bonded to an elastic–ideally plastic core on a rigid foundation. After core yielding, the problem is separated into an outer region where the core is elastic and an inner region where the core exerts a constant reactive pressure on the face sheet. The outer region is modeled as a plate on an elastic foundation. The inner region is modeled using small-deflection plate theory, first-order large-deflection plate theory, and membrane theory. The unknown plastic radius is found by matching the boundary conditions for the two regions. The extension of the model to orthotropic face sheets is indicated and demonstrated by examples. The predictions are in close agreement with experiments, which contrasts to previously published models where membrane effects and core crushing were neglected. The model can be used for improved modeling of impact on sandwich panels.

I. Introduction

IMPACTS on sandwich panels with laminated face sheets can result in substantial strength reductions and face-sheet delaminations similar to those observed in monolithic laminates. Studies of the problem have been reviewed by Tsang[1] and are, in most cases, experimental works aimed at determining damage size relative to impact energy. Analytical models[2–7] of the impact response of sandwich panels have, with two exceptions,[2,6] been based on empirically determined static load–indentation relations. The static indentation of sandwich panels has been studied experimentally[3–9] and analytically[6–8,10] using small-deflection theory and an assumed elastic core behavior. In most cases the predictions were in poor agreement with experiments, except for the early part of the loading. In practice, core-cell crushing and face-sheet deflections much larger than the face-sheet thickness are observed. In the present work, core crushing and large face-sheet deflections are incorporated in a simplified dimensionless theory for contact indentation of sandwich panels, resulting in a significantly improved description of typical experiments.

II. Problem Definition

The problem under consideration is to determine the load-indentation relation for an elastic hemispherical body indenting a sandwich panel. The model assumes axisymmetry and considers a concentrated load on an elastic, infinite face sheet resting on a core that is bonded to a rigid foundation. The core is assumed elastic in tension but elastic–ideally plastic in compression, which is a reasonable approximation for the observed behavior of typical core materials.[11] The face sheet, of thickness h, is characterized by the inplane modulus E_r, Poisson's ratio ν_r, and plate bending stiffness D_r. The core, of thickness h_c, is characterized by the elastic foundation stiffness k and compressive yield stress p_0. The coupling between deformations resulting from bending, shear, and Hertzian indentation of the face sheet is neglected. After core yielding, the problem can be separated in two models as shown in Fig. 1.

Presented as Paper 95-1374 at the AIAA/ASME/ASCE/AHS/ASC Structures, Structural Dynamics, and Materials Conference, New Orleans, LA, April 10–12, 1995; received July 29, 1995; revision received Feb. 19, 1996; accepted for publication March 2, 1996.

*Research Assistant, Department of Aeronautics and Astronautics; currently Researcher, Aeronautical Research Institute of Sweden, P.O. Box 11021, Bromma S-161 11, Sweden.

†Class of 1943 Assistant Professor. Senior Member AIAA.

For convenience, we use the following simplified notation for the face-sheet elastic properties, stress resultants, displacements, and slope:

$$\begin{aligned} D_r &\to D, & Q_r(a) &\to Q \\ E_r &\to E, & M_r(a) &\to M \\ \nu_r &\to \nu, & N_r(a) &\to N \\ w(0) &\to w, & w(a) &\to w_a \\ u_r(a) &\to u, & \frac{\mathrm{d}w(a)}{\mathrm{d}r} &\to -\theta \end{aligned} \tag{1}$$

We also define the following dimensionless quantities:

$$L_0^4 = D/k \tag{2}$$

$$\bar{a} = \sqrt{p_0 \pi a^2 / F} \tag{3}$$

$$\bar{F} = \frac{F}{p_0 \pi L_0^2} \tag{4}$$

$$\bar{M} = \frac{M}{p_0 L_0^2} \tag{5}$$

$$\rho = r/L_0 \tag{6}$$

$$\rho_a = a/L_0 = \bar{a}\sqrt{\bar{F}} \tag{7}$$

Here ρ is a general dimensionless radius, $\bar{a}$ is the dimensionless plastic radius, $\bar{F}$ is the dimensionless contact force, $\bar{M}$ is the dimensionless edge moment at $r = a$, and L_0 is a characteristic length dependent on the plate stiffness and foundation stiffness.

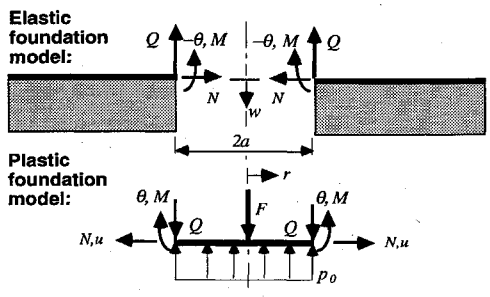

Fig. 1 Substructuring of the model problem.

III. Plate Solution for Small Deflections

A general theory for Kirchhoff plates on a shear deformable foundation is given in Ref. 12, and a theory for a shear deformable plate can be found in Ref. 13. When shear deformation is neglected, the equilibrium equation for axisymmetric deformation of a plate on an elastic foundation can be written in the following dimensionless form[12]:

$$\Delta_\rho^2 w(\rho) + w(\rho) = q/k \tag{8}$$

where $\Delta_\rho = d^2/d\rho^2 + \rho^{-1}d/d\rho$, where q is the load applied on the upper surface of the plate. The maximum deflection under a point load on an infinite plate is given by[12]

$$w(0) = \tfrac{1}{8}F/\sqrt{kD} \tag{9}$$

After core yielding, the point load is excluded from the elastically supported region and the deformation is governed by the homogeneous version of Eq. (8). The reactive pressure p in the elastic area is given by $p = kw$. Hence, after core yielding, the deflection w_a at the elastic–plastic transition radius will be given by

$$w_a = p_0/k \tag{10}$$

where p_0 is the compressive yield stress of the core. The critical load at initiation of core yielding is obtained by combining Eqs. (9) and (10):

$$F_{cr} = 8p_0L_0^2 \tag{11}$$

The general solution to the homogeneous differential equation, Eq. (8) is given by[12]

$$w(\rho) = C_1u_0(\rho) + C_2v_0(\rho) + C_3f_0(\rho) + C_4g_0(\rho)$$

where

$$\begin{aligned} u_n(\rho) + iv_n(\rho) &= J_n(\rho\sqrt{i}) \\ f_n(\rho) + ig_n(\rho) &= H_n^{(1)}(\rho\sqrt{i}) \end{aligned} \tag{12}$$

The real functions u_n, v_n, f_n, and g_n are the real and imaginary parts of the nth-order Bessel function J_n and nth-order Hankel function of the first kind, $H_n^{(1)}$.

For an infinite plate, a bounded solution forces the constants C_1 and C_2 to be zero, and the solution takes the following form[12,14]:

$$w(\rho) = w_a[\bar{C}_3f_0(\rho) + \bar{C}_4g_0(\rho)] \tag{13}$$

$$\frac{dw}{dr} = -\frac{w_a}{L_0}\sum_{i=3}^{4}\bar{C}_i\theta_i(\rho) \tag{14}$$

$$M_r = \frac{w_aD}{L_0^2}\sum_{i=3}^{4}\bar{C}_i[M_i(\rho) - (1-\nu)\bar{M}_i(\rho)] \tag{15}$$

$$Q_r = -\frac{w_aD}{L_0^3}\sum_{i=3}^{4}\bar{C}_iQ_i(\rho) \tag{16}$$

where

$$\bar{C}_i = C_i/w_a = C_ik/p_0 \tag{17}$$

where M_r is the moment and Q_r is the shear force on surfaces normal to the radius. The functions f_0, g_0, θ_i, M_i, $\bar{M}_i$, and Q_i are given by

$$\begin{aligned} f_n &= \mathrm{Re}H_n^{(1)}(\rho\sqrt{i}) = -(2/\pi)(-1)^n kei_n\rho \\ g_n &= \mathrm{Im}H_n^{(1)}(\rho\sqrt{i}) = -(2/\pi)(-1)^n ker_n\rho \\ \theta_3 &= \frac{f_1 - g_1}{\sqrt{2}}, \qquad \theta_4 = \frac{f_1 + g_1}{\sqrt{2}} \\ M_3 &= -g_0, \qquad M_4 = f_0 \\ \bar{M}_3 &= \theta_3/\rho, \qquad \bar{M}_4 = \theta_4/\rho \\ Q_3 &= -\theta_4, \qquad Q_4 = \theta_3 \end{aligned} \tag{18}$$

Here ker_n and kei_n are the real and imaginary parts of Kelvin functions.[14] Tables of f_n and g_n can be found in Ref. 13.

The unknown constants and the plastic radius can be determined by matching three of the expressions in Eqs. (13–16) with corresponding expressions for the inner region. The bending solution w_b for the inner region is obtained by superposition of standard solutions[15] for the bending deflection attributable to a central point load, a uniform pressure, and an edge moment on a simply supported plate, which, by use of the dimensionless quantities in Eqs. (2–7), can be written

$$w_b = \frac{F^2\bar{a}^2}{16\pi^2p_0D(1+\nu)}[(3+\nu) - \bar{a}^2(5+\nu)/4 + 8\bar{M}/\bar{F}] \tag{19}$$

$$\theta = \frac{F\rho_aL_0}{8\pi D(1+\nu)}(2 - \bar{a}^2 + 8\bar{M}/\bar{F}) \tag{20}$$

The edge shear force Q is obtained from vertical equilibrium of the inner plate region:

$$Q = \frac{(\bar{a}^2 - 1)F}{2\pi a} \tag{21}$$

After core yielding, the compatibility conditions at the plastic radius are

$$w(a_+) = w(a_-) = w_a \tag{22}$$

$$\theta(a_+) = \theta(a_-) \tag{23}$$

$$Q(a_+) = Q(a_-) \tag{24}$$

Now, the three unknowns $\bar{C}_3$, $\bar{C}_4$, and ρ_a can be determined from the three compatibility equations (22–24). Equations (13–22) immediately give

$$\bar{C}_4 = \frac{1 - \bar{C}_3f_0}{g_0} \tag{25}$$

Matching shear loads, Eqs. (21) and (16), and using Eqs. (2–7) and (25), we find

$$\bar{C}_3 = \frac{[(\bar{F}/\rho_a - \rho_a)/2 - (Q_4/g_0)]}{Q_3 - Q_4f_0/g_0} \tag{26}$$

Matching slopes, Eqs. (20) and (14), and using Eqs. (2–7), we finally get the following dimensionless equation relating ρ_a to $\bar{F}$:

$$\begin{aligned} &\bar{C}_3[M_3 - (1-\nu)\bar{M}_3] + \bar{C}_4[M_4 - (1-\nu)\bar{M}_4] \\ &\quad + (2\bar{F} - \rho_a^2)/8 = (1+\nu)[\bar{C}_3\theta_3 + \bar{C}_4\theta_4]/\rho_a \end{aligned} \tag{27}$$

The solution to Eq. (27) was obtained by numerical iteration to find $\bar{F}$ for different values of the argument ρ_a. Poisson's ratio affects the resulting edge moment, but no effect was seen on the plastic radius.

IV. Additional Sources of Flexibility

The additional displacements attributable to shear deformation w_s and the approach α between the face sheet and indentor attributable to contact stresses become significant for small plate deflections.

The approach α and contact radius c between the indentor of radius R and the face-sheet backface attributable to contact stresses are given by[16]

$$\alpha = (F/k_\alpha)^{\frac{2}{3}}$$

where

$$\begin{aligned} k_\alpha &= \tfrac{4}{3}Q_\alpha\sqrt{R} \\ 1/Q_\alpha &= 1/Q_1 + 1/Q_2 \end{aligned} \tag{28}$$

$$c = \sqrt{R\alpha} \tag{29}$$

The out-of-plane stiffnesses Q_1 of the face sheet and Q_2 of the indentor are given by

$$Q_i = E_i/(1 - \nu_i^2) \tag{30}$$

For laminated anisotropic face sheets the out-of-plane stiffness and modulus are approximately equal.[16]

As shown in Ref. 14, the shear deformation w_s in the inner region is obtained by superposition of the shear attributable to a uniform pressure[15] and a concentrated load[17] uniformly distributed inside a small radius c:

$$w_s = \frac{(1 - 4\nu_{rz}G_{rz}/E_r)\left[1 - \bar{a}^2/8 + \frac{3}{4}\ell_n(a/c)\right] - \bar{a}^2/4}{\pi G_{rz}h} F \quad (31)$$

After core yielding, the total center deflection is given by

$$w = \alpha + w_a + w_b + w_s \quad (32)$$

V. Plate Solution for Large Deflections

Increasing deflections increase both the magnitude and the vertical component of the membrane stresses, resulting in a geometrically nonlinear load–deflection relation. Significant deviations from small-deflection theory are seen for deflections in the order of the face sheet thickness. The small-deflection solution is based on linear theory, although core crushing results in a nonlinear load–displacement relation. Here the terms linear and nonlinear solution are used to refer to solutions based on small- and large-deflection theory. If shear is neglected, we obtain[18] the following type of relations between the loads in the linear (F_L) and first-order nonlinear (F_{NL}) solutions for a given deflection:

$$\bar{F}_{NL}/\bar{F}_L = 1 + \bar{k}_m\bar{w}^2 \qquad \text{where} \qquad \bar{w} = w/h \quad (33)$$

Here $\bar{k}_m$ is a dimensionless membrane stiffness that depends on the boundary conditions and the type of load. The present problem involves the combination of a central point load and a uniform reactive pressure as well as rotational and radial-edge constraints. No general analytical solution was found to this problem, and solutions for a combined point load and uniform pressure on a circular plate were found only for clamped boundary conditions.

In the following, an approximate solution is obtained by consideration of the constraints on the edge of the plastic region and linear interpolation between the solutions for clamped and hinged edges that are either radially sliding or fixed. The dimensionless membrane stiffnesses for clamped conditions are obtained from the second term in published series solutions.[19,20] Approximate expressions for the hinged cases can be derived[14] from the clamped cases by adding a correction corresponding to the vertical component of the edge stress. Here, only the final expressions are given.

1) Edges in sliding clamps ($N = 0, \theta = 0$):

$$\bar{k}_{m1} = \frac{1 - \nu^2}{10{,}800}(1212\lambda^3 + 4409\lambda^2 - 388\lambda + 2190) \quad (34)$$

where $\lambda = \beta/(1 + 4\beta)$ and $\beta = F/(q\pi a^2)$. In the present problem, $q = -p_0$ and $\beta = -1/\bar{a}^2$.

2) Edges in fixed clamps ($u = 0, \theta = 0$):

$$\bar{k}_{m2} = 48(1 - \nu^2)\left[\beta^3\left(\frac{1}{8}\alpha_1 - \frac{47}{81}\right) + \frac{1}{36}\beta^2 \times\left(\alpha_2 + \frac{5}{4}\alpha_1 - \frac{791}{64}\right) + \frac{1}{96}\beta\left(\alpha_3 + \frac{20}{27}\alpha_2 - \frac{953}{150}\right) + \frac{1}{1728}\left(5\alpha_3 - \frac{77}{10}\right)\right]\Big/(1 + 4\beta)^3 \quad (35)$$

where

$$\alpha_1 = (9 - 7\nu)/(1 - \nu)$$

$$\alpha_2 = (16 - 11\nu)/(1 - \nu)$$

$$\alpha_3 = (5 - 3\nu)/(1 - \nu)$$

3) Edges in sliding hinges ($N = 0, M = 0$):

$$\bar{k}_{m3} = \bar{k}_{m1} \quad (36)$$

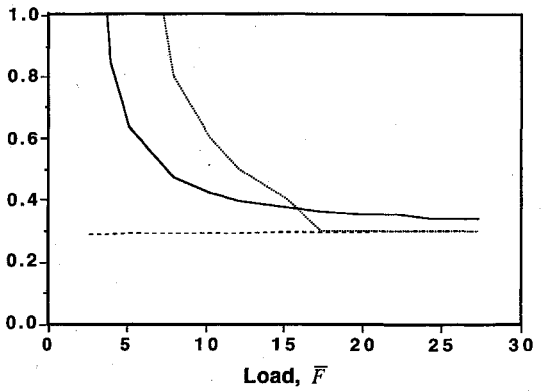

Fig. 2 Functions for large-deflection plate solution: ·····, μ; ——, $\bar{k}_m$; and - - - -, $\bar{k}_{mcl}$.

4) Edges in fixed hinges ($u = 0, M = 0$):

$$\bar{k}_{m4} = \bar{k}_{m2} + 3(2 - \bar{a}^2)/4 \quad (37)$$

The expression for $\bar{k}_{m4}$ in Ref. 14 has been corrected. Note that $\bar{a}^2 = 2$ corresponds to zero edge moment and slope. For a point load ($\bar{a}^2 = 0$) the stiffness for sliding hinges is in close agreement with published closed-form solutions whereas the stiffness for fixed hinges is 37–56% higher than the closed-form solutions.[18,21]

5) Combined edge constraints ($N \neq 0, M \neq 0$). The dimensionless membrane stiffness $\bar{k}_{mcl}$ for the radially constrained clamped case is obtained by linear interpolation between the fixed- and sliding-edge cases:

$$\bar{k}_{mcl} = \bar{k}_1 + \left(\frac{N}{N_{fixed}}\right)[\bar{k}_{m2} - \bar{k}_{m1}] \quad (38)$$

where the ratio N/N_{fixed} is assumed to be equal to σ/σ_{fixed} in Eq. (53). The stiffness $\bar{k}_{mhi}$ in the hinged case is obtained by an analogous interpolation between cases 3 and 4. The membrane stiffness for the rotationally and radially constrained case is finally calculated by linear interpolation between the hinged and clamped cases:

$$\bar{k}_m = \bar{k}_{mhi} + (\bar{M}/\bar{M}_{cl})(\bar{k}_{mcl} - \bar{k}_{mhi}) \quad (39)$$

where $\bar{M}_{cl} = \bar{a}^2 - 2$. Here $\bar{M}_{cl}$ is the edge moment in a clamped plate. After consideration of the change in plastic radius[14] attributable to the increased edge load, the relation between the loads for the linear and nonlinear solutions is given by

$$\bar{F}_{NL}/\bar{F}_L = \sqrt{(1 + \bar{k}_m\bar{w}^2)/[1 + (\bar{k}_m - \bar{k}_{mcl})\bar{w}^2]^{\mu}} \quad (40)$$

where the exponent μ is given by the local slope in a log–log plot of the plastic radius vs load. Here, it is assumed that both dimensionless loads are defined using the plastic radius given by Eq. (27). The functions of Eq. (40) are shown in Fig. 2.

VI. Membrane Solution

For large deflections ($w/h > 1$) the face-sheet stress state will gradually be dominated by the membrane stress σ_r (Fig. 3). The major membrane effect obviously will come from the inner region because slopes in the outer region are small. We model the face sheet in the inner region as a pure membrane, while continuing to model the surrounding face sheet as a plate.

Vertical equilibrium for the inner region is given by

$$F - p_0\pi a^2 - 2\pi a\sigma h\theta = 0 \quad (41)$$

The boundary conditions at the plastic radius are

$$w(a_-) = w(a_+) = w_a \quad (42)$$

$$M(a_-) = M(a_+) = 0 \quad (43)$$

$$\sigma_r(a_-)h\theta = -Q(a_+) \quad (44)$$

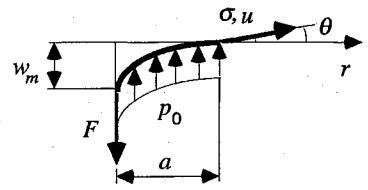

Fig. 3 Membrane under combined loading.

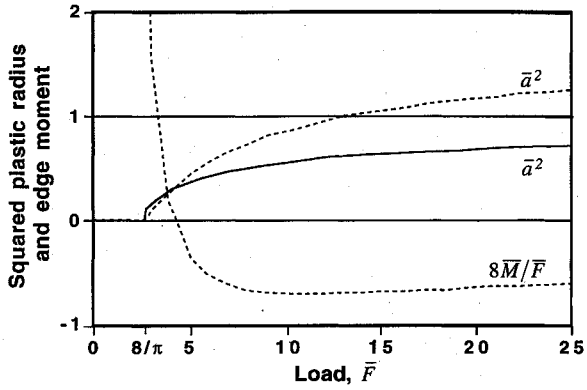

Fig. 4 Edge moment and plastic radius for $\nu = 0.3$: ----, plate; and ——, membrane.

because membranes are unable to carry moments and shear. Equations (13–17) are still valid for the outer, elastically supported, region. The displacement condition at the plastic radius and thus the relation between $\bar{C}_3$ and $\bar{C}_4$ in Eq. (25) remains unchanged. Satisfaction of Eq. (43) together with Eq. (15) and use of Eqs. (2–7) gives an additional equation from which the constant $\bar{C}_3$ can be solved:

$$1/\bar{C}_3 = f_0 - \frac{g_0[\bar{M}_3 - (1-\nu)\bar{M}_3]}{M_4 - (1-\nu)\bar{M}_4} \tag{45}$$

Combination of Eqs. (16) and (41) with the boundary condition in Eq. (44), rearrangement of terms, and use of Eqs. (2) and (7) finally gives the following equation for dimensionless plastic radius vs load:

$$\frac{\bar{F}/\rho_a - \rho_a}{\bar{C}_3(Q_3 - Q_4 f_0/g_0) + Q_4/g_0} = 2 \tag{46}$$

In Fig. 4 the dimensionless plastic radius of the membrane solution for $\nu = 0.3$ has been compared with the corresponding dimensionless radius and edge moment of the plate solution.

To calculate the membrane deflections in the inner region, we must determine the constraint from the surrounding face sheet. The general solution for an axisymmetric membrane stress state is given by[22]

$$\begin{aligned} \sigma_r &= A_1/r^2 + A_2(1 + 2\ln r) + 2A_3 \\ \sigma_\varphi &= -A_1/r^2 + A_2(3 + 2\ln r) + 2A_3 \end{aligned} \tag{47}$$

If plane stress conditions are assumed, the radial strain is given by

$$\varepsilon_r = \frac{\mathrm{d}u_r}{\mathrm{d}r} = \frac{\sigma_r - \nu\sigma_\varphi}{E} \tag{48}$$

The boundary conditions for the outer region are

$$\sigma_r(a) = \sigma;\ \sigma_r(r) \quad \text{and} \quad u_r(r) \to 0 \quad \text{as} \quad r \to \infty \tag{49}$$

Satisfying the stress condition in Eq. (49) at infinity forces the constants A_2 and A_3 to vanish. By solving for the constant A_1, we obtain the following expressions for the stresses:

$$-\sigma_\varphi = \sigma_r = \sigma(a/r)^2 \qquad \text{for} \qquad r \geq a \tag{50}$$

By inserting Eq. (50) into Eq. (48), integrating, and satisfying the displacement condition in Eq. (49), we obtain the expression for the radial displacement in the outer region. At the plastic radius, we obtain the following stress–displacement relation:

$$(u/a)/(\sigma/E) = -(1+\nu) \tag{51}$$

The radial edge constraint on the inner region in the plate solution can be estimated by considering a uniform stress state $\sigma_r = \sigma_\varphi = \sigma$. The total membrane strain attributable to constrained edges and a uniform stress state in the inner region is then obtained by adding the strain resulting from the edge displacement prescribed in Eq. (51) to the strain in the case with fixed edges, which results in the following relation:

$$(1-\nu)(\sigma/E) = (1-\nu)(\sigma_{\text{fixed}}/E) - (1+\nu)(\sigma/E) \tag{52}$$

where σ is the radial-edge stress in the case with radially constrained edges and σ_{fixed} is the stress when the edges are fixed. By solving for the radial-edge stress σ, we obtain the following relation for a radially constrained membrane in uniform plane stress:

$$\sigma/\sigma_{\text{fixed}} = (1-\nu)/2 \tag{53}$$

A general solution for a point load on an initially flat membrane with a prescribed relation between edge displacement and edge stress is given in Ref. 23, which also includes an experimental verification. The deflection in the case of interacting loads cannot be obtained through superposition of the single-load cases, because of the nonlinear nature of the membrane equations. However, the solution for a point load represents an upper bound for the deflection in the combined-load case. The inclusion of a reactive pressure in the solution for a point load[23] is associated with significant mathematical difficulties.

In the following, an approximate solution is derived using the Ritz method, which gives a lower bound of the exact solution for the combined-load case. A previous version of the solution[14,24] is improved here by omitting the simplifying assumption of a uniform stress state. For simplicity the assumed deflection shape is given by a second-order polynomial, which describes the shape of a cable under a constant load per unit length.[25] After consideration of the condition of zero deflection at the membrane edge, the assumed deflection shape can be written

$$w(s) = [1 + C(s - s^2) - s^2]w_m \tag{54}$$

where $s = r/a$. Here, w_m is the central membrane deflection attributable to the combined load, and C is a shape parameter. The radial displacement u_r is assumed to be a linear function of the edge deflection u:

$$u_r = ru/a \tag{55}$$

Assuming small strains and rotations, the kinematic relations of the membrane are given by[15]

$$\begin{aligned} \varepsilon_r &= \frac{\mathrm{d}u_r}{\mathrm{d}r} + \frac{1}{2}\left(\frac{\mathrm{d}w}{\mathrm{d}r}\right)^2 \\ \varepsilon_\varphi &= u_r/r \end{aligned} \tag{56}$$

Assuming plane stress, the constitutive relations of the membrane are given by[22]

$$\sigma_r = \frac{E(\varepsilon_r + \nu\varepsilon_\varphi)}{1-\nu^2} \tag{57}$$

For a linearly elastic material and plane stress, the total potential energy Π of the membrane is given by[22]

$$\Pi = U - W$$

where

$$\begin{aligned} U &= \frac{1}{2E}\int_0^\infty (\sigma_r^2 + \sigma_\varphi^2 - 2\nu\sigma_r\sigma_\varphi)2\pi hr\,\mathrm{d}r \\ W &= Fw_m - \int_0^a p_0 w(r)2\pi hr\,\mathrm{d}r \end{aligned} \tag{58}$$

where U is the internal strain energy and W is the work done by external forces. The final expression for the work function is obtained by integration and use of Eqs. (3) and (54):

$$W = Fw_m[1 - \bar{a}^2(3 + C)/6] \tag{59}$$

For small rotations, $dw/dr \ll 1$, the horizontal equilibrium equation in Ref. 23 simplifies to

$$\sigma_\varphi = \sigma_r + r\frac{d\sigma_r}{dr} \tag{60}$$

where $\sigma_i = N_i/h$. By use of Eq. (60), the strain energy U in Eq. (57) can be expressed in the following form:

$$U = \frac{\pi h}{E}\int_0^\infty \left[(1-\nu)\frac{d}{dr}(r^2\sigma_r^2) + r^3\left(\frac{d\sigma_r}{dr}\right)^2\right]dr \tag{61}$$

The stress in the outer region is now given by Eq. (50). The stress in the inner region can be expressed in terms of the displacements u and w_m through Eqs. (54–57). The edge displacement u can be expressed in terms of the edge stress σ by the use of Eq. (51). Finally, the edge stress can be expressed solely in terms of the displacement w_m by evaluating the resulting stress expression at the plastic radius and solving for σ. The resulting strain energy expression then can be written:

$$U = \frac{\pi E h w_m^4}{(1-\nu^2)^2 a^2}\left[(C+1)^2\frac{7C^2+32C+40}{15} + (1-\nu)^2\frac{(2+C)^4}{8}\right] \tag{62}$$

By inserting Eqs. (59) and (62) in Eq. (58), we obtain an expression for the potential energy of the membrane. Differentiating with respect to w_m and equating to zero, we obtain the following expression for the central deflection:

$$w_m = f_w\left(\frac{F^2\bar{a}^2}{2p_0 Eh}\right)^{\frac{1}{3}}$$

where

$$f_w^3 = \frac{(1-\nu^2)^2[1-\bar{a}^2(3+C)/6]/(2\pi^2)}{(7C^2+32C+40)(C+1)^2/15 + (1-\nu)^2(2+C)^4/8} \tag{63}$$

The constant C can be determined as a function of the dimensionless plastic radius by differenting the potential energy with respect to C and equating the resulting expression to zero, which gives the following equation:

$$\frac{1}{Fw_m}\frac{\partial \Pi}{\partial C} = \frac{f_w^3\pi^2}{(1-\nu^2)^2}\left[(C+1)\frac{14C^2+55C+56}{15} + (1-\nu)^2\frac{(2+C)^3}{4}\right] + \frac{\bar{a}^2}{6} = 0 \tag{64}$$

The above equation is solved for C by iteration, and the value of the function f_w is calculated. Note that f_w is, in effect, a reduction factor to the solution for a point load with no reactive pressure, where f_w should be equal to unity. The edge slope angle is obtained by evaluation of the derivative of Eq. (54) at the plastic radius ($s = 1$):

$$\theta = -\left.\frac{dw}{dr}\right|_{s=1} = \frac{(2+C)w_m}{a} \tag{65}$$

Note that the physical limits of θ correspond to a value of C in the range $-2 \le C \le -1$. The function f_w and the normalized edge slope angle $\theta/(w_m/a)$ for $\nu = 0.3$ are shown in Fig. 5.

According to the membrane theory, a point load will result in a noncontinuous slope (a cusp) at the origin (Fig. 6). In practice, the load is distributed over a small area and locally the radius of curvature of a perfect membrane will be equal to the indentor tip radius. The contact radius can be estimated by equating the slopes of the indentor surface and the assumed membrane shape. A simple expression[14] for the contact radius r_1 is obtained under the assumption that it is small in comparison to both the plastic radius and the indentor tip radius. For true membranes, no Hertzian contact will occur. Thus, the total membrane deflection after removal of the cusp is given by

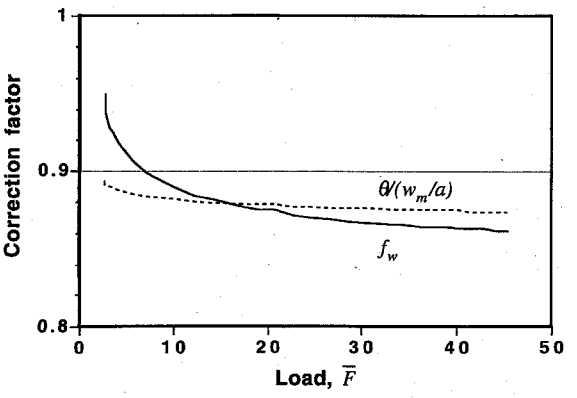

Fig. 5 Membrane deflection and edge slope normalized by the point load solution.

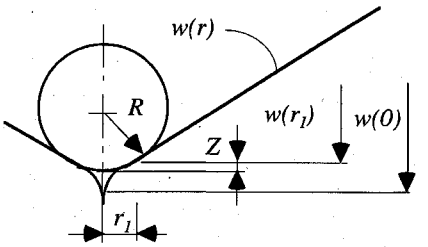

Fig. 6 Geometry under the indentor.

$$\begin{aligned} w_{mcorr} &= w_a + w(r_1) + Z(r_1) \\ &= w_a + w_m - \tfrac{1}{2}R(Cw_m/a)^2 \end{aligned} \tag{66}$$

where the last term represents the cusp correction. In practice, the assumption of a comparatively small contact radius is often violated, which requires a more complex expression for the last term of Eq. (66).

VII. Additional Considerations

An approximate solution for orthotropic face sheets can be obtained by length scaling[14] and use of the following effective plate stiffness:

$$\begin{aligned} \bar{D}^* &= \left\{\frac{\pi/2}{K[\sqrt{(1-A)/2}]}\right\}^2, \qquad 0 \le A \le 1 \\ \bar{D}^* &= \left\{\frac{(\pi/4)(A+1)}{K[\sqrt{(A-1)/(A+1)}]}\right\}^2, \qquad 1 < A \end{aligned} \tag{67}$$

where $\bar{D}^* = D^*/\sqrt{(D_x D_y)}$ and $A = D_{xy}/\sqrt{(D_x D_y)}$. $K(s)$ is the complete elliptic integral of the first kind. The effective membrane properties are given by their average in-plane values.

The foundation stiffness in the present[14] one-dimensional core model is given by

$$k = Q_c/h_c^* \tag{68}$$

where $h_c^* = \min\langle h_c, h_c^{3D}\rangle$. The core stiffness Q_c is defined as in Eq. (30). The effective core thickness h_c^* is limited by h_c^{3D}, which is an equivalent thickness obtained when matching[14] the displacement in Eq. (9) to the corresponding three-dimensional solution[26] for a plate on an elastic half-space:

$$h_c^{3D} = \tfrac{128}{27}(2D/Q_c)^{\frac{1}{3}} \tag{69}$$

Bounds for the residual indentation can be obtained by considering the energy lost in plastic deformation.[14]

VIII. Results and Discussion

If the deformation attributable to shear and Hertzian contact are neglected, then the load–displacement relation can be put in a

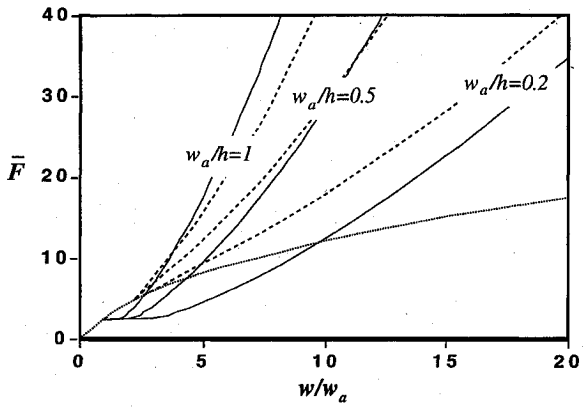

Fig. 7 Comparison of load–indentation solutions: ---, plate, nonlinear; ——, membrane; and · · · ·, plate, linear.

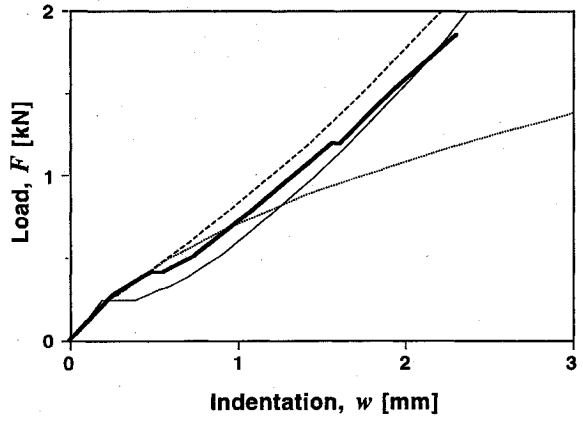

Fig. 8 Comparison with experiment by Tsang (Ref. 7): ---, plate, nonlinear; ▬, experiment; ——, membrane; and · · · ·, plate, linear.

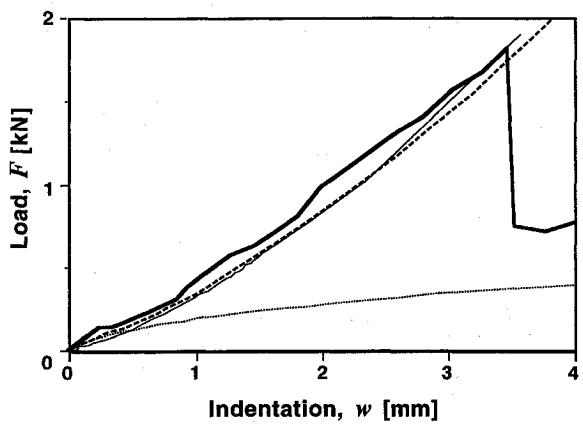

Fig. 9 Comparison with experiment by Williamson and Lagace (Ref. 9): ▬, experiment; ---, plate, nonlinear; ——, membrane; and · · · ·, plate, linear.

simple dimensionless form by normalizing with the indentation required for core yielding. In Fig. 7 the membrane and plate solutions are compared for some different values of the critical indentation. The load history generally consists of three segments: an initial linear part prior to core yielding at the critical load $\bar{F}_{cr} \approx 2.5$, followed by a softening, and later a gradual membrane stiffening for larger deflections. The small-deflection plate solution is applicable for deflections up to one face-sheet thickness, whereas the membrane solution represents an asymptotic solution for much larger deflections. The large-deflection plate solution can be applied for intermediate deflections.

A good agreement was generally found when comparing[14] the solution with several published experimental studies.[3,5,7,9] In Fig. 8 the theory is compared with an indentation experiment on a panel with 0.8-mm graphite–epoxy face sheets on a 12.7-mm rigid foam core.[7] In accompanying impact experiments, delaminations occurred at an impact load of 1.5 kN and fiber failure occurred at about 1.8 kN. In Fig. 9 the theory is compared with an indentation experiment on a panel with 0.35-mm woven graphite–epoxy face sheets on a 25.4-mm Nomex® core.[9] In this case the thin face sheet allows very large deflections before penetration at 1.8 kN, and the entire behavior can be described by the membrane solution.

A limited parametric study[14] based on the present model indicates that the load–indentation behavior is governed primarily by the core-crush stress and face-sheet thickness. The influence of core modulus and thickness diminishes quickly after initiation of core yielding.

The present model predicts the peak indentation and core-crush diameter, which are important parameters when predicting[1] the postimpact compressive behavior of sandwich panels. The model was recently extended[27] to predict initiation and growth of face-sheet damage. The fact that delaminations prior to fiber failure do not significantly change the membrane stiffness of the face sheet was used to predict indentation behavior and subsequent fiber failures after initiation of face-sheet delamination.

IX. Conclusions

Because of their low core strength and thin face sheets, sandwich panels under indentation usually undergo core yielding and large face-sheet deflections. The incorporation of these phenomena in the present model significantly improves predictions of the load–indentation behavior when compared with previous models assuming small deflections and elastic core behavior. The fairly linear relation between load and indentation observed in many experiments is explained by the combined effect of face-sheet membrane stiffening and core softening attributable to yielding.

Future work should include a more rigorous membrane analysis and an investigation of the relation between the present one-dimensional core model and three-dimensional analysis.

Acknowledgments

This work was funded by the Swedish Defence Materials Administration. The authors also are indebted to M. Landahl, who contributed valuable advice and suggestions during the work.

References

[1]Tsang, P. H. W., "Impact Resistance and Damage Tolerance of Composite Sandwich Panels," Ph.D. Thesis, Dept. of Aeronautics and Astronautics, Massachusetts Inst. of Technology, Cambridge, MA, Feb. 1994.

[2]Nemes, J. A., and Simmonds, K. E., "Low-Velocity Impact Response of Foam-Core Sandwich Composites," *Journal of Composite Materials*, Vol. 26, No. 4, 1992, pp. 500–519.

[3]Mines, R. A. W., Worrall, C. M., and Gibson, A. G., "The Response of GRP Sandwich Panels to Dropped Object Impact Loading," *Fibre Reinforced Composites, FRC'90* (Liverpool, England, UK), Mechanical Engineering Publications, Suffolk, England, UK, 1990, pp. 149–155.

[4]Lee, L. J., Huang, K. Y., and Fann, Y. J., "Dynamic Responses of Composite Sandwich Plate Impacted by a Rigid Ball," *Journal of Composite Materials*, Vol. 27, No. 13, 1993, pp. 1238–1256.

[5]Sun, C. T., and Wu, C. L., "Low Velocity Impact of Composite Sandwich Panels," *Proceedings of the AIAA 32nd Structures, Structural Dynamics, and Materials Conference* (Baltimore, MD), AIAA, Washington, DC, 1991, pp. 1123–1129 (AIAA Paper 91-1077).

[6]Lie, S. C., "Damage Resistance and Damage Tolerance of Thin Composite Facesheet Honeycomb Panels," M.S. Thesis, Dept. of Aeronautics and Astronautics, Massachuetts Inst. of Technology, Cambridge, MA, March 1989.

[7]Tsang, P. H. W., "Impact Resistance of Graphite/Epoxy Sandwich Panels," M.S. Thesis, Dept. of Aeronautics and Astronautics, Massachusetts Inst. of Technology, Cambridge, MA, Aug. 1989.

[8]Slepetz, J. M., Oplinger, D. W., Parker, B. S., and Tremblay, R. T., "Impact Damage Tolerance of Graphite/Epoxy Sandwich Panels," U.S. Air Force Materials and Mechanics Research Center, AMMRC TR 74-20, Watertown, MA, Sept. 1974.

[9]Williamson, J. E., and Lagace, P. A., "Response Mechanisms in the Impact of Graphite/Epoxy Honeycomb Sandwich Panels," *Proceedings of the American Society for Composites Eighth Technical Conference* (Cleveland, OH), Technomic, Lancaster, PA, 1993, pp. 287–297.

[10]Ericsson, A., and Sankar, B. V., "Contact Stiffness of Sandwich Plates and Application to Impact Problems," *Proceedings of the Second International Conference on Sandwich Construction* (Gainesville, FL), Engineering Materials Advisory Services, Solihull, England, UK, 1992, pp. 139–159.

[11]Gibson, L. J., and Ashby, M. F., *Cellular Solids*, Pergamon, Oxford, England, UK, 1988, Chaps. 4 and 5.

[12]Vlasov, V. Z., and Leont'ev, U. N., "Beams, Plates and Shells on Elastic Foundations," Israel Program for Scientific Translations, Jerusalem, 1966 (original Russian edition, 1960), Chap. 4.

[13]Panc, V., *Theories of Elastic Plates*, Noordhoff International, Leyden, The Netherlands, 1975, pp. 581–591.

[14]Olsson, R., "Simplified Theory for Contact Indentation of Sandwich Panels," FFA TN 1994-33, Aeronautical Research Inst. of Sweden, Bromma, 1994; M.S. Thesis, Dept. of Aeronautics and Astronautics, Massachusetts Inst. of Technology, Cambridge, MA, 1994.

[15]Timoshenko, S., and Woinowsky–Krieger, S., *Theory of Plates and Shells*, 2nd ed., McGraw–Hill, New York, 1959, Chaps. 3 and 13.

[16]Olsson, R., "Impact Response of Orthotropic Composite Laminates Predicted from a One-Parameter Differential Equation," *AIAA Journal*, Vol. 30, No. 6, 1992, pp. 1587–1596.

[17]Shivakumar, K. N., Elber, W., and Illg, W., "Prediction of Impact Force and Duration Due to Low-Velocity Impact on Circular Composite Laminates," *Journal of Applied Mechanics*, Vol. 52, No. 3, 1985, pp. 674–680.

[18]Volmir (Wolmir), A. S., *Biegsame Platten und Schalen*, Verlag für Bauwesen, Berlin, 1962 (corrected German edition of 1961 Russian edition), Chap. 4.

[19]Schmidt, R., and DaDeppo, D. A., "Large Axisymmetric Deflections of a Loosely Clamped Circular Plate Subjected to a System of Two Interacting Loads," *Industrial Mathematics*, Vol. 26, No. 1, 1976, pp. 11–16.

[20]Saibel, E., and Tadjbakhsh, I., "Large Deflections of Circular Plates Under Uniform and Concentrated Loads," *Zeitschrift für Angewandte Mathematik und Physik*, Vol. 11, No. 6, 1960, pp. 496–503.

[21]Banerjee, B., "Large Deflection of a Circular Plate Under a Concentrated Load—A New Approach," *Industrial Mathematics*, Vol. 33, No. 1, 1983, pp. 57–61.

[22]Timoshenko, S., and Goodier, J. N., *Theory of Elasticity*, 2nd ed., McGraw–Hill, New York, 1951, pp. 20, 58, and 148.

[23]Jahsman, W. E., Field, F. A., and Holmes, A. M. C., "Finite Deformations in a Prestressed, Centrally Loaded, Circular Elastic Membrane," *Proceedings of the 4th U.S. National Congress of Applied Mechanics*, American Society of Mechanical Engineers, Berkeley, CA, 1962, pp. 585–594.

[24]Olsson, R., and McManus, H. L., "Simplified Theory for Contact Indentation of Sandwich Panels," *Proceedings of the AIAA 36th Structures, Structural Dynamics and, Materials Conference* (New Orleans, LA), AIAA, Washington, DC, 1995, pp. 1812–1820 (AIAA Paper 95-1374).

[25]Leonard, J. W., *Tension Structures—Behavior and Analysis*, McGraw–Hill, New York, 1988, pp. 35, 36.

[26]Sneddon, I. N., Gladwell, G. M. L., and Coen, S., "Bonded Contact of an Infinite Plate and an Elastic Foundation," *Letters in Applied and Engineering Sciences*, Vol. 3, No. 1, 1975, pp. 1–13.

[27]Olsson, R., "Prediction of Impact Damage in Sandwich Panels," *Proceedings of the Third International Conference on Sandwich Construction* (Southampton, England, UK), Engineering Materials Advisory Services, Solihull, England, UK, 1995, pp. 659–668; FFA TN 1995-35, Aeronautical Research Inst. of Sweden, Bromma, Sweden.